Angewandte International Edition Chemie

DOI: 10.1002/anie.201302655

Organoboron Surface Chemistry

Facile Monolayer Formation on SiO_2 Surfaces via Organoboron Functionalities**

*Arunava Agarwala, Thangavel Subramani, Amir Goldbourt, David Danovich, and Roie Yerushalmi**

Organoboron surface functionalities are widely used in the contexts of sensing,[1] catalysis,[2] chromatography,[3] and surface doping,[4] among others. Several studies have demonstrated the introduction of organoboron surface functionalities through attachment by molecular linking groups: the linker group with the organoboron moiety attached at one end undergoes a reaction at its other end to form a covalent bond to the surface.[4a,5] There are very few examples, however, of the modification of surfaces by the direct attachment of a boron functionality to the interface.[2b] The organoboron modification of oxides, such as silica nanoparticles (SiO_2 NPs) and Si/SiO_2 interfaces, is attractive for a wide range of applications. Therefore, a facile method for the direct anchoring of organoboron functionalities to SiO_2 surfaces is desirable.

Herein we present the formation of boron-containing monolayers on SiO_2 by the direct treatment of surface silanol groups (Si−OH) with the boron functionality. The direct reaction of an organoboron with SiO_2 was studied for dichlorophenylborane (**B1**) and chlorodicyclohexylborane (**B2**; Scheme 1). Monolayer formation was observed under mild conditions on SiO_2 nanoparticles and Si/SiO_2 surfaces. Surface modifications of SiO_2 NPs were characterized by FTIR spectroscopy, X-ray photoelectron spectroscopy (XPS), thermogravimetric analysis (TGA), and solid-state ^{11}B and ^{13}C NMR spectroscopy and modeled by density functional theory (DFT) computational analysis. Monolayer formation was also studied for Si/SiO_2 wafers by ellipsometry, contact-angle (CA) and atomic force microscopy (AFM). The as-prepared monolayers exhibited selective reactivity towards diols in accord with the expected reactivity of the boron moiety; no reactivity towards monoalcohols was observed. SiO_2 NPs modified with **B1** and **B2** were thermally annealed and characterized to identify the thermal-degradation products and boron species formed upon monolayer decomposition at elevated temperatures. Our results showed that both **B1** and **B2** react with surface silanol groups within a few minutes at room temperature. The reaction with **B1** yielded mainly the surface form Si−O−B(−Ph,−OH), whereas the reaction with **B2** yielded a mixture of surface species, including Si−O−B($-C_6H_{11}$,−OH), because of partial cleavage of the organic moieties. High-temperature treatment of the modified SiO_2 NPs led to decomposition of the organic moieties and boron incorporation into the SiO_2 framework to form borosiloxane (B−O−Si) bridges.

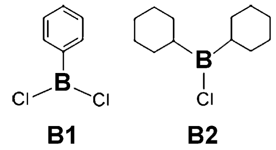

Scheme 1. Organoboron precursors used in this study.

SiO_2 NPs that had reacted with **B1** showed IR absorption peaks at approximately 3100 cm^{-1}, which were assigned to the ν(C−H) mode of the phenyl ring (Figure 1a). The bands at 1352 and 1369 cm^{-1} were assigned to ν(B−O).[6] The sharp peaks at 1441 and 1603 cm^{-1} indicated the presence of an aryl group bonded to boron.[6a] The peak at 700 cm^{-1} was assigned to an out-of-plane C−H deformation. Furthermore, a minor peak at 1632 cm^{-1} suggested the presence of surface-adsorbed water molecules.[7] For annealing temperatures above 300 °C, significant changes in the FTIR spectra were observed. These changes are expected and result from decomposition of the organic moiety and additional processes that occur at the surface, as discussed below.

For annealing temperatures above 300 °C, all IR bands associated with ν(C−H), as well as the bands associated with the aryl functionality, were completely removed (Figure 1a), and an increase in the band at 825 cm^{-1} was observed owing to the formation of Si−O−Si species at the surface.[8] Furthermore, the two peaks at 1352 and 1369 cm^{-1} observed at low temperatures (≤ 300 °C) evolved to a broad band at 1396 cm^{-1} indicative of B−O species that persist to the highest temperatures investigated in this study.

---

[*] Dr. A. Agarwala, Dr. T. Subramani, Dr. R. Yerushalmi
Institute of Chemistry and Center for Nanoscience and Nanotechnology, The Hebrew University of Jerusalem
Edmond J. Safra Campus, Givat Ram, Jerusalem, 91904 (Israel)
E-mail: roie.yerushalmi@mail.huji.ac.il
Dr. A. Goldbourt
School of Chemistry, Raymond and Beverly Sackler Faculty of Exact Sciences, Tel Aviv University
Ramat Aviv, Tel Aviv, 69978 (Israel)
Dr. D. Danovich
Institute of Chemistry and Lise Meitner Minerva Center for Computational Quantum Chemistry, The Hebrew University of Jerusalem
Edmond J. Safra Campus, Givat Ram Jerusalem, 91904 (Israel)

[**] We thank Prof. David Avnir for assistance in TGA measurements and Dr. Vitaly Gutkin for XPS analysis. This research was partially funded by a starting grant from the European Research Council (ERC) under the Seventh Framework Programme of the European Community (Grant agreement no 259312) and the Farkas Center for Light-Induced Processes (R.Y.). The NMR spectrometer was partially funded by the Tel Aviv Center for Nanosciences and Nanotechnology.

Supporting information for this article is available on the WWW under http://dx.doi.org/10.1002/anie.201302655.

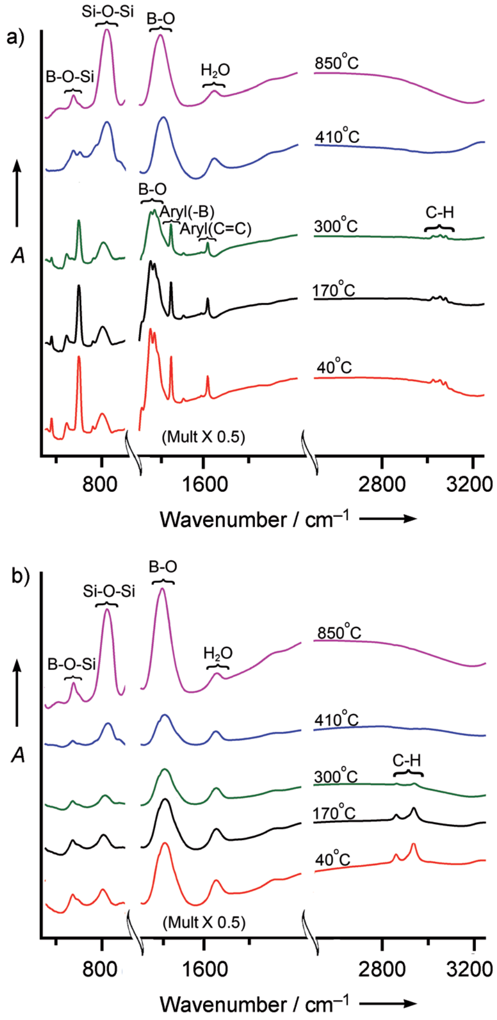

Figure 1. FTIR spectra of SiO_2 NPs treated with a) **B1** and b) **B2**. Samples were annealed in air at the specified temperatures.

SiO_2 NPs that had undergone reaction with **B2** showed IR absorption peaks at 2860 and 2935 cm^{-1} assigned to the aliphatic ν(C–H) mode (Figure 1 b). In contrast to **B1**–SiO_2, the ν(B–O) mode was observed as a broad band at 1408 cm^{-1} at annealing temperatures from 40 °C; this band was similar to the high-temperature peaks observed for **B1**–SiO_2 at temperatures above 300 °C. The aliphatic ν(C–H) peaks completely disappeared for temperatures above 300 °C, whereas the ν(B–O) band at 1408 cm^{-1} increased in intensity and shifted to 1396 cm^{-1}. The band at 675 cm^{-1} assigned to Si–O–B species was enhanced at high annealing temperatures, which may suggest the incorporation of boron species into the SiO_2 framework at elevated temperatures.[8,9a] Additionally, the IR spectra obtained for **B1**–SiO_2 and **B2**–SiO_2 samples annealed at 410 and 850 °C were highly similar, which suggests the presence of similar surface species at these annealing temperatures for both types of monolayers studied.

The boron species present at the various annealing temperatures were characterized further by ^{13}C and ^{11}B magic-angle spinning (MAS) solid-state NMR spectroscopy. ^{13}C NMR cross-polarization signals were observed for both types of monolayers. These signals verified the presence of phenyl and cyclohexyl groups on the **B1**–SiO_2 and **B2**–SiO_2 NPs, respectively (see the Supporting Information for more details). Line shapes obtained from ^{11}B spin-echo MAS NMR spectroscopic experiments (Figure 2) are the combined result of the isotropic chemical shifts and the second-order quadrupolar couplings. Therefore, chemical shifts were extracted from full line-shape simulations (see Figure S2 A in the Supporting Information). For trigonal species, these shifts can be read to a good approximation from the high-frequency edge of the ^{11}B spectrum. Overall, the ^{11}B NMR spectra demonstrated primarily trigonal boron species, with some amount of tetrahedral boron species formed at the higher temperatures (the proportion of tetrahedral species may be underestimated herein owing to the selective excitation inherent to the spin-echo pulse sequence employed). For SiO_2 NPs treated with **B1** and **B2**, the ^{11}B chemical-shift values ruled out the presence of halogenated (B–Cl) species, the chemical shifts of which are expected at 50–80 ppm (Figure 2), and suggested the existence of B–OH species, typically observed at 25–35 ppm,[10] in line with the FTIR spectroscopic results and XPS data (see below). Furthermore, $R_2B(OH)$ species were expected to show higher chemical shifts than those observed in this study, which suggests for as-prepared samples the form Si–O–B(–R,–OH), in which R = phenyl and C_6H_{11} for **B1** and **B2**, respectively.[11] The change in line shape and position ($\delta \approx 19$ ppm) of the peak in the ^{11}B NMR spectrum of **B2**–SiO_2 NPs annealed at 170 °C suggests that new species were formed with a trigonal boron environment, whereas for **B1**–SiO_2 only a slight broadening of the peak was observed with no significant change in line shape in comparison to that of the peak for the as-prepared sample.

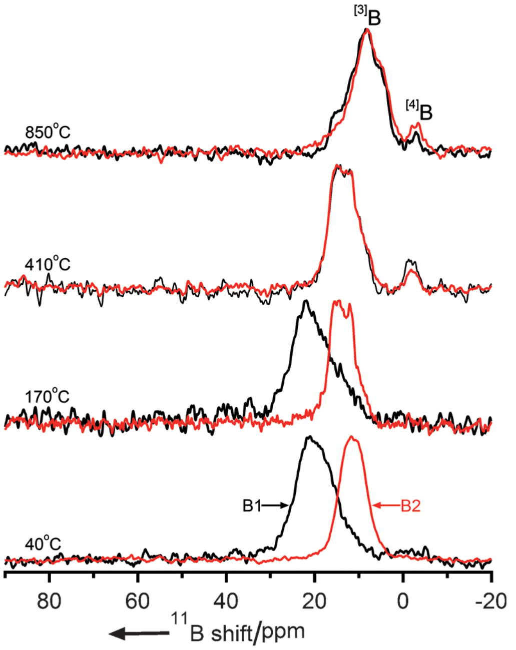

Figure 2. ^{11}B spin-echo MAS NMR spectra of SiO_2 NPs treated with **B1** (black) and **B2** (red). Samples were annealed in air at the specified temperatures. Trigonal ([3]B) and tetracoordinated ([4]B) boron species are indicated.

At 410 °C, both **B1**–SiO_2 and **B2**–SiO_2 samples exhibit similar spectra with chemical shifts of 19 ppm and a quadrupolar coupling constant of approximately 2.6 MHz. These values are highly similar to those reported for boroxyl ring BO_3 species (17.5 ppm, 2.65 MHz) in borosilicates[12] and for extraframework $B(OH)_3$ groups in boron-doped zeolite β[13] or in boron-modified MCM-41.[14] At the highest annealing temperature in this study, 850 °C, a further shift was observed in the spectra, and although the line shapes suggested that at least two boron species were present, the clear trigonal site at 13 ppm confirms the anchoring of ^{11}B atoms to the framework on the basis of its similarity to that observed upon boroxyl-ring opening[12] or the conversion of $B(OH)_3$ species into $B(OH)_n(OSi)_{3-n}$ species.[13–15] The shoulder at a higher shift indicates residual extraframework boron species. Above 400 °C, tetracoordinated boron species were observed at around 0 ppm. These species indicate the penetration of boron into the silica framework and were assigned as $B(OB)(OSi)_3$ at 410 °C ($\delta = 0$ ppm) and $B(OSi)_4$ at 850 °C ($\delta \approx -2$ ppm).[12a] Overall, the spectra collected for the **B1**–SiO_2 and **B2**–SiO_2 samples annealed at 410 and 850 °C are highly similar, in line with the FTIR results.

Thermal decomposition of the **B1**–SiO_2 and **B2**–SiO_2 samples was studied by TGA–XPS (Figure 3). A weight change indicative of the adsorption of water molecules was observed at approximately 100 °C in both cases. Decomposition of the organic components was indicated by weight changes commencing at approximately 400 and 300 °C for **B1** and **B2**, respectively. The C 1s XPS signal decreased for both **B1**–SiO_2 and **B2**–SiO_2 samples at elevated temperatures, with almost no carbon retained at 1005 °C (Figure 3 a,b, open circles). In contrast, a significant portion of the boron was retained at high annealing temperatures, as indicated by the B 1s XPS signal at 1005 °C, which had about 65 and 40 % of the initial intensity for **B1**–SiO_2 and **B2**–SiO_2, respectively (Figure 3 a,b, open rectangles). These results together with the NMR and IR spectroscopic results suggest the incorporation of boron species into the oxide framework. The C/B ratio for the modified NPs prior to thermal annealing yielded the expected value of 6 for **B1**–SiO_2 and a lower than expected value for **B2**–SiO_2, in agreement with ^{11}B NMR chemical-shift data, which already indicated the absence of $R_2B(OH)$ species at 40 °C. Furthermore, the differential thermal gravimetry peak areas in the thermal-decomposition region was significantly higher for **B1**–SiO_2 than for **B2**–SiO_2 (Figure 3 a,b). Collectively, the XPS and TGA results further support partial cleavage of the cyclohexyl moiety at low temperatures for **B2**–SiO_2, whereas for **B1**–SiO_2 the phenyl moiety is retained up to 300 °C. Further support of this observation comes from the ^{13}C NMR spectra, in which **B1**–SiO_2 NPs readily gave the expected signal, whereas the intensity of the signal for **B2**–SiO_2 NPs annealed at 170 °C is significantly lower (see Figure S2 B). The XPS B 1s binding energies exhibited a sharp increase from 192.7 to 194.0 eV for **B1**–SiO_2, whereas a constant value of 193.7 eV was observed for **B2**–SiO_2 (Figure 3 c). The sharp increase in binding energy for **B1** occurred concomitantly with the cleavage of the phenyl ring. Thus, it appears that there is a change in the boron chemical environment, with more BO_x species present at elevated temperatures.[9] This result is in line with the thermal evolution of the ^{11}B NMR and FTIR spectra, which showed two distinct chemical environments for the two types of monolayers formed by **B1**–SiO_2 and **B2**–SiO_2 at low temperatures and identical species following thermal annealing at high temperatures. Furthermore, the characterization methods applied in this study, including XPS, ^{11}B NMR spectroscopy, and FTIR spectroscopy, showed more pronounced changes in the boron chemical environment upon thermal annealing for **B1**–SiO_2 than for **B2**–SiO_2, probably because of the facile cleavage of the cyclohexyl moieties. This result is also in line with the expected trend in the stabilization of the boron–carbon bonds by the aryl and alkyl substituents owing to π back donation in the case of the phenyl substituent.[16]

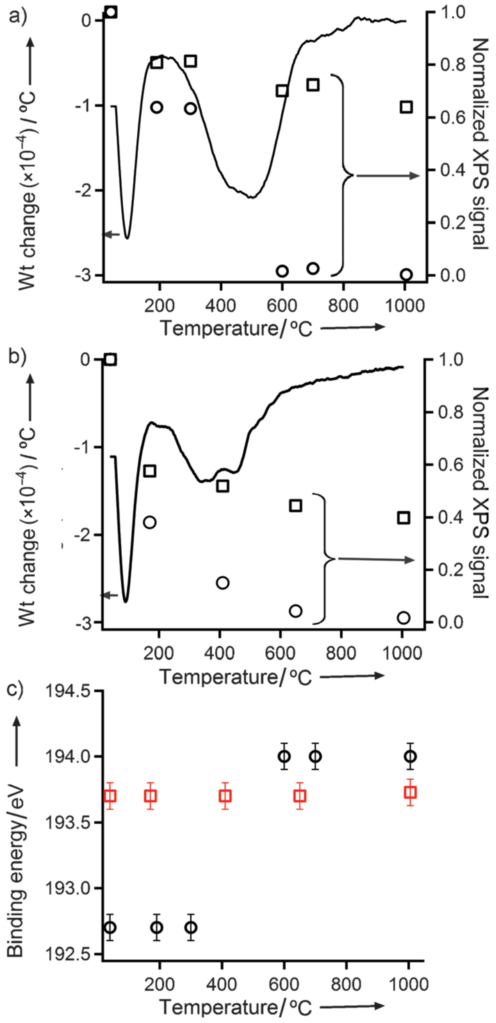

Figure 3. a,b) Differential thermal gravimetry profiles and X-ray photoelectron spectroscopy (XPS) data: B 1s (□) and C 1s (○) normalized signals for **B1**- (a) and **B2**-treated SiO_2 NPs (b) annealed at various temperatures. c) Plot of the binding energy (B 1s component) versus the annealing temperature for samples with **B1** (○) and **B2** (□) monolayers formed on SiO_2 nanoparticles. See the Supporting Information for B 1s XPS spectra.

The surface reactions of **B1** and **B2** with SiO_2 were complete at room temperature within 10 min, which suggests that the reaction is barrier-free or has a very low activation energy. Computational analysis (see Figures S3 and S4) suggested that the reaction of neutral Si−OH species with **B1** and **B2** involves activation energies of approximately 14 kcal mol^{-1}, depending on the reaction details. In contrast, the reaction coordinates for the zwitterionic form $-\mathrm{SiO}^{(-)},\mathrm{SiOH}_2^{(+)}$ yield a barrier-free path to the observed products. This result is in line with the acid–base character of $\mathrm{SiO_2}$ surfaces.[17] Furthermore, monolayer formation with both **B1** and **B2** provides −BOH surface species as basic surface sites (p$K_a \approx 7$–9) that may further promote the surface reaction.

The reactivity of freshly prepared **B1**–$\mathrm{SiO_2}$ NPs towards alcohols was studied for ethanol, phenol, catechol, ethylene glycol, 1,3-propanediol, and 1,4-butanediol in anhydrous 1,4-dioxane (75 mM, 60 °C, 2 h; see the Supporting Information for additional details). The observed disappearance of the B−O vibration band following reactions with the diols indicated the removal of B−O species from the surface. The reaction with catechol resulted in a partial decrease in the intensity of the B−O band, whereas reactions with ethanol and phenol did not affect the IR spectra (see Figure S5). These results suggest selective reactivity of the **B1**–$\mathrm{SiO_2}$ NPs towards diols.

Experimental Section

Surface modification of $\mathrm{SiO_2}$ NPs: 15 nm $\mathrm{SiO_2}$ NPs (100 mg) and a mesitylene solution of the appropriate precursor, **B1** or **B2** (77 mM; 5 mL), were placed in a 20 mL screw-cap vial, and the vial was sealed tightly. The reaction mixture was kept at a temperature between room temperature and 100 °C for a length of time between 10 min and 2 h. Immediately after the reaction, the monolayer-coated $\mathrm{SiO_2}$ NPs were removed from the solution of the precursor by centrifugation, the supernatant phase was discarded, and the NPs were washed with mesitylene and redispersed in mesitylene 3 times, then washed with *n*-hexane and redispersed in *n*-hexane twice, and finally dried at 115 °C. All solutions were prepared, reactions were set up, and samples were handled in a $\mathrm{N_2}$ glove box.

Thermogravimetric analysis (TGA) was performed with a Mettler-Toledo 851e system. Differential thermal gravimetry profiles were calculated from the data by the use of STARe software. Experiments were performed over the temperature range of 40–1005 °C with a ramp rate of 10 °C min^{-1} and a 50 mL min^{-1} flow of dry $\mathrm{N_2}$.

Spin-echo ^{11}B magic-angle spinning solid-state NMR spectroscopy was performed on a 14.1 Tesla Avance III Bruker spectrometer with a 4 mm wide-bore probe and corrected for the background ^{11}B signal. For more details, see the Supporting Information.

Monolayer formation was characterized by variable-angle spectroscopic ellipsometry (VASE) with a VB-400 spectroscopic ellipsometer (J. A. Woolam Co.). Ellipsometry measurements performed on a Si(100) substrate with native oxide yielded (4 ± 1) and (3 ± 1) Å for **B1** and **B2**, respectively. Monolayer formation was also characterized by atomic force microscopy (AFM), which showed no aggregate formation (see Figure S6 in the Supporting Information). Contact-angle measurements performed with an Attension instrument yielded a water contact angle of (39 ± 5) and (35 ± 5)° for **B1**- and **B2**-modified surfaces, respectively.

Received: March 30, 2013

Keywords: boranes · monolayers · nanoparticles · silica · surface modification

[1] a) W. Liu, M. Pink, D. Lee, *J. Am. Chem. Soc.* **2009**, *131*, 8703–8707; b) C. Vahlberg, M. Linares, P. Norman, K. Uvdal, *J. Phys. Chem. C* **2012**, *116*, 796–806; c) W. Huang, K. Besar, R. LeCover, A. M. Rule, P. N. Breysse, H. E. Katz, *J. Am. Chem. Soc.* **2012**, *134*, 14650–14653; d) J. Yoon, A. W. Czarnik, *J. Am. Chem. Soc.* **1992**, *114*, 5874–5875.

[2] a) E. U. X. Chen, T. J. Marks, *Chem. Rev.* **2000**, *100*, 1391–1434; b) Y. J. Wanglee, J. Hu, R. E. White, M. Y. Lee, S. M. Stewart, P. Perrotin, S. L. Scott, *J. Am. Chem. Soc.* **2012**, *134*, 355–366; c) N. Millot, A. Cox, C. C. Santini, Y. Molard, J. M. Basset, *Chem. Eur. J.* **2002**, *8*, 1438–1442; d) S. Krackl, A. Company, Y. Aksu, D. Avnir, M. Driess, *ChemCatChem* **2011**, *3*, 227–232.

[3] S. Mohapatra, N. Panda, P. Pramanik, *Mater. Sci. Eng. C* **2009**, *29*, 2254–2260.

[4] a) J. C. Ho, R. Yerushalmi, Z. A. Jacobson, Z. Fan, R. L. Alley, A. Javey, *Nat. Mater.* **2008**, *7*, 62–67; b) J. C. Ho, R. Yerushalmi, G. Smith, P. Majhi, J. Bennett, J. Halim, V. N. Faifer, A. Javey, *Nano Lett.* **2009**, *9*, 725–730.

[5] a) D. Barriet, C. M. Yam, O. E. Shmakova, A. C. Jamison, T. R. Lee, *Langmuir* **2007**, *23*, 8866–8875; b) O. Abed, M. Wanunu, A. Vaskevich, R. Arad-Yellin, A. Shanzer, I. Rubinstein, *Chem. Mater.* **2006**, *18*, 1247–1260.

[6] a) G. Socratts, *Infrared and Raman Characteristic Group Frequencies: Tables and Charts*, Wiley, Chichester, **2010**; b) G. D. Soraru̇, N. Dallabona, C. Gervais, F. Babonneau, *Chem. Mater.* **1999**, *11*, 910–919.

[7] a) X. Li, W. Li, Z. Zuang, Z. Zong, Q. Li, L. Wang, *J. Phys. Chem. C* **2012**, *116*, 16047–16053; b) V. M. Bermudez, J. T. Robinson, *Langmuir* **2011**, *27*, 11026–11036.

[8] Q. Wang, L. Fu, X. Hu, Z. Zhang, Z. Xie, *J. Appl. Polym. Sci.* **2006**, *99*, 719–724.

[9] a) L. Bois, P. L'Haridon, Y. Laurent, X. Gouin, P. Grange, J.-F. Letard, J. M. Birot, J.-P. Pillot, J. Dunogues, *J. Alloys Compd.* **1996**, *232*, 244–253; b) O. M. Moon, B. C. Kang, C. B. Lee, J. H. Boo, *Thin Solid Films* **2004**, *464–465*, 164–169.

[10] J. W. E. Weiss, D. L. Bryce, *J. Phys. Chem. A* **2010**, *114*, 5119–5131.

[11] a) G. W. Kramer, H. C. Brown, *J. Organomet. Chem.* **1974**, *73*, 1–15; b) J. E. DeMoor, G. P. Van der Kelen, *J. Organomet. Chem.* **1966**, *6*, 235–241.

[12] a) L. S. Du, J. F. Stebbins, *J. Phys. Chem. B* **2003**, *107*, 10063–10076; b) L.-S. Du, J. F. Stebbins, *J. Non-Cryst. Solids* **2003**, *315*, 239–255.

[13] H. Koller, C. Fild, R. F. Lobo, *Microporous Mesoporous Mater.* **2005**, *79*, 215–224.

[14] A. Sayari, I. Moudrakovski, C. Danumah, C. I. Ratcliffe, J. A. Ripmeester, K. F. Preston, *J. Phys. Chem.* **1995**, *99*, 16373–16379.

[15] I. Eswaramoorthi, A. K. Dalai, *Microporous Mesoporous Mater.* **2006**, *93*, 1–11.

[16] a) V. Bachler, N. Metzler-Nolte, *Eur. J. Inorg. Chem.* **1998**, 733–744; b) Y. Yamamoto, I. Moritani, *J. Org. Chem.* **1975**, *40*, 3434–3437.

[17] In one study it was found that the −SiOH groups of fused silica exhibited pK_a values ranging from about 4 to about 9, depending on the silanol microscopic environment: Md. S. Azam, C. N. Weeraman, J. M. Gibbs-Davis, *J. Phys. Chem. Lett.* **2012**, *3*, 1269–1274.